JOURNAL OF MATERIALS SCIENCE 22 (1987) 2893–2898

A thermodynamical approach to chemical vapour deposition of TiC and TiN on superalloys

A. TELAMA, K. TORKKELL, T. MÄNTYLÄ, P. KETTUNEN
Institute of Materials Science, Tampere University of Technology, PO Box 527, SF-33101 Tampere, Finland

Thermodynamical calculations have been used to predict the interaction of surface and gas phase during chemical vapour deposition of TiC and TiN on superalloys. Calculated equilibrium data were used to interpret the problems encountered during deposition and to optimize process parameters for two superalloy compositions. The calculations indicated that in certain conditions the formation of Ni_3Ti, liquid $CrCl_2$ and liquid $FeCl_2$ is possible. These compounds were presumed to be one reason for the poor adhesion and open structure of the coatings observed in some experiments. An Ni_3Ti interlayer and traces of $CrCl_2$ were also found experimentally. The superalloys used in this study were the nickel-based ODS alloy MA 6000 and the iron-based alloy Incoloy 800.

1. Introduction

The interaction between the substrate and the gas phase at the beginning of the chemical vapour deposition (CVD) process has an effect on many important properties of the final coating. Chemical reactions between an aggressive gas phase and substrate constituents may yield molten compounds which will destroy locally the adherence of the coating or will cause vigorous evaporation of volatile compounds which may hinder locally the growth of the coating. Prediction of these reactions is difficult if the substrate material is composed of several elements. One estimate of possible reactions between substrate materials and gas phase can be obtained by thermodynamical calculations.

Some thermodynamical calculations for TiC have already been done [1–4], but according to our knowledge thermodynamics has not been used to predict the interaction between substrate material and gas phase in CVD of TiC or TiN. The purpose of this study is to compare the results of thermodynamical calculations with the experimental results and in that way check if thermodynamical calculations can be used to optimize CVD parameters.

2. Thermodynamical calculations

The computer program SOLGASMIX developed by Erikson [5] was used for the equilibrium calculations. This program is based on minimizing the total free energy of the system by the method of Lagrangian undetermined multiplers.

For thermodynamical modelling of the CVD system the following presumptions were made:

1. The deposition system is closed and homogeneous.
2. Thermodynamical equilibrium is not limited by reaction kinetics.
3. No impurities exist (leakage, oxide layers on samples, reaction chamber does not take part in the reactions).
4. Gas phase and solutions are ideal.
5. MA 6000 (a nickel based alloy) is modelled by a solution of nickel, chromium, iron and aluminium. The alloying elements of MA 6000 such as tantalum, molybdenum and tungsten were ignored in thermodynamical calculations for calculation simplicity. They would probably have the same kind of effect, even though not so strong, as aluminium. Incoloy 800 (an iron-based alloy) is modelled by a solution of iron, nickel and chromium. Compositions of these materials are listed in Table I.

All components considered in equilibrium calculations are listed in Table II.

Since the local conditions in the vicinity of the surface may differ considerably from the conditions in the other parts of the reactor, the calculations were performed with an excess of substrate material (100 times more metal species of substrate than gaseous reactants) in input reactants, with an excess of gaseous species (100 times) in input reactants, and with equal inputs. The results of these calculations were compared with experimentally observed results.

2.1. Titanium carbide on MA 6000 and on Incoloy 800

Thermodynamical calculations suggest that the deposition rate could be increased if there exist species which are effective reducers for $TiCl_4$. This is especially true for aluminium, which forms very stable chlorides. If the calculations are performed in conditions where $TiCl_4$ is effectively reduced, a nickel–titanium intermetallic compound, Ni_3Ti, is obtained.

The most significant difference between the CVD equilibrium diagrams calculated having a metal excess or having a gas excess in input reactants is that in the case of metal excess equilibrium Ni_3Ti is obtained

0022–2461/87 $03.00 + .12

TABLE I Composition of MA 6000 and Incoloy 800

Alloy	Composition (wt %)								
	Fe	Ni	Cr	Al	W	Ti	Mo	Ta	Y_2O_3
MA 6000	1	bal	15	4	4	2	2	2	1
Incoloy 800	bal	31	20						

only at temperatures below 1350 K. If the calculations are performed with a gas excess in input reactants, Ni_3Ti is obtained only at temperatures above 1285 K. Fig. 1 shows the TiC–MA 6000 system equilibrium for equal inputs of metals and gases in input reactants.

At high $CH_4/TiCl_4$ input ratios chromium carbides are present in equilibrium diagrams. If the calculations are carried out using a metal excess in input reactants, formation of chromium carbides is shifted to higher $CH_4/TiCl_4$ ratios, since excessive aluminium reduces $TiCl_4$ very effectively. The increased amount of titanium available reacts with carbon and the increased yield of TiC decreases the yield of less stable carbides. Fig. 2 shows the yield of some solid compounds obtained from different $CH_4/TiCl_4$ input ratios.

According to the calculations the iron-based alloy Incoloy 800 is less prone to Ni_3Ti formation. This was thought to be caused by the fact that it contains less nickel and because there is no aluminium present. Lack of aluminium means that less titanium chlorides are reduced as compared to MA 6000. Fig. 3 shows the equilibrium diagram for the system TiC–Incoloy 800.

TABLE II Substances considered in equilibrium calculations and sources of thermochemical data

Substance	Reference	Substance	Reference
$H_2(g)$	[6]	$H(g)$	[6]
$Cl_2(g)$	[6]	$Cl(g)$	[6]
$HCl(g)$	[6]	$TiCl_4(g)$	[6]
$TiCl_3(g)$	[6]	$TiCl_2(g)$	[6]
$TiCl(g)$	[6]	$NiCl_2(g, s)$	[6]
$FeCl(g)$	[6]	$FeCl_2(g, l)$	[6]
$FeCl_3(g)$	[6]	$Fe_2Cl_6(g)$	[6]
$CH_4(g)$	[6]	$CH_3(g)$	[6]
$CH_2(g)$	[6]	$C_2H_2(g)$	[6]
$C_2Cl_4(g)$	[6]	$CH_3Cl(g)$	[8]
$CCl(g)$	[6]	$CCl_3(g)$	[6]
$CCl_2(g)$	[6]	$AlCl(g)$	[6]
$AlCl_2(g)$	[6]	$AlCl_3(g)$	[6]
$Al_2Cl_6(g)$	[6]	$N_2(g)$	[6]
$N(g)$	[6]	$NH_3(g)$	[6]
$N_2H_4(g)$	[6]	$CN(g)$	[6]
$C_2N_2(g)$	[6]	$CrCl_2(l, s)$	[6]
$CrCl_3(s)$	[6]	$Cr_2N(s)$	[6]
$CrN(s)$	[6]	$AlN(s)$	[6]
$TiN(s)$	[6]	$TiC(s)$	[6]
$Cr_{23}C_6(s)$	[6]	$Cr_7C_3(s)$	[6]
$Cr_3C_2(s)$	[6]	$Al_4C_3(s)$	[6]
$Fe_3C(s)$	[6]	$TiH_2(s)$	[6]
$Ti(s)$	[6]	$Ni(s)$	[6]
$Fe(s)$	[6]	$Cr(s)$	[6]
$C(s)$	[6]	$Al(l, s)$	[6]
$TiNi_3(s)$	[7]	$TiNi(s)$	[7]
$Ti_2Ni(s)$	[7]	$TiAl_3(s)$	[7]
$TiAl(s)$	[7]	$Ti_3Al(s)$	Estimated
$TiFe_2(s)$	[7]	$TiFe(s)$	[7]
$Ni_3Al(s)$	[7]	$NiAl(s)$	[7]
$Ni_2Al_3(s)$	[7]	$NiAl_3(s)$	[7]

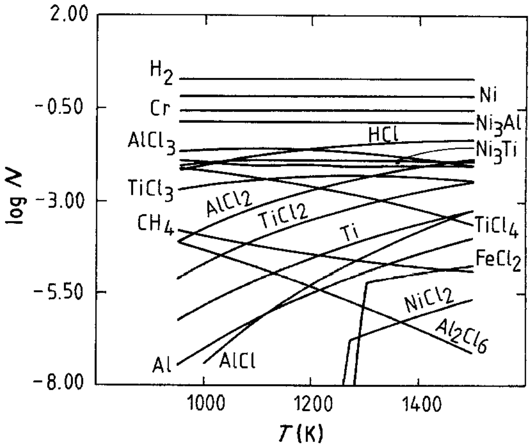

Figure 1 Yield of components as a function of temperature in the system TiC–MA 6000; $p = 1$ atm, metal/gas ratio of inputs = 1 ($N_{Ni} = 1.15$ mol, $N_{Cr} = 0.29$ mol, $N_{Al} = 0.16$ mol, $N_{Fe} = 0.01$ mol, $N_{TiCl_4} = 0.03$ mol, $N_{CH_4} = 0.01$ mol, and $N_{H_2} = 2.00$ mol).

2.2. Titanium nitride on MA 6000 and Incoloy 800

When the deposition of TiN on MA 6000 is analysed, calculations indicate that besides aluminium also chromium takes part in reduction reactions of titanium chlorides. This means that liquid chromium chloride ($CrCl_2$) can be formed. If the amount of hydrogen is decreased, the formation of chromium chlorides is shifted to higher temperatures and liquid iron chloride is also formed.

The most significant difference between the deposition of TiC and TiN is that in the case of TiN the Ni_3Ti phase is not formed due to the following reasons: TiN is more stable than TiC, the $H_2/TiCl_4$ ratio is smaller for TiN than for TiC and the $CH_4/TiCl_4$ ratio in CVD of TiC is smaller than the $N_2/TiCl_4$ ratio in CVD of TiN. Excessive nitrogen allows chromium nitride to be formed at low temperatures. The equilibrium diagram for the system TiN–MA 6000 is shown in Fig. 4. The equilibrium diagram for the system TiN–Incoloy is very similar to that for TiN–MA 6000.

3. Experimental procedure

TiC and TiN coatings were produced in a hot-wall type laboratory CVD installation according to the

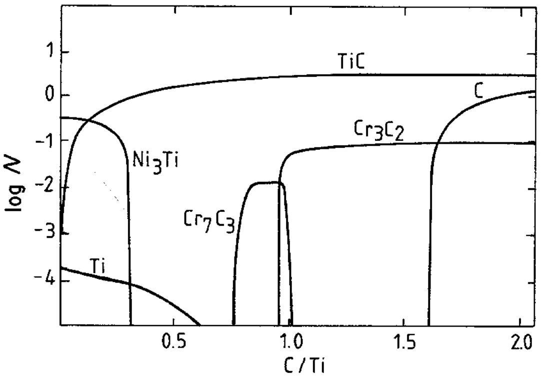

Figure 2 Yield of some solid compounds as a function of $CH_4/TiCl_4$ ratio in the system TiC–MA 6000; $p = 1$ atm, $T = 1273$ K, gas excess in input reactants ($N_{Ni} = 1.15$ mol, $N_{Cr} = 0.29$ mol, $N_{Al} = 0.16$ mol, $N_{Fe} = 0.01$ mol, $N_{TiCl_4} = 3.0$ mol and $N_{H_2} = 200$ mol).

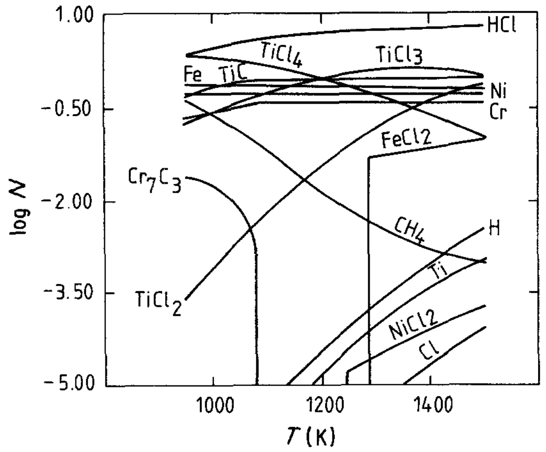

Figure 3 Yield of components as a function of temperature in the system TiC–Incoloy; $p = 1$ atm, gas excess in input reactants ($N_{Fe} = 0.76$ mol, $N_{Ni} = 0.55$ mol, $N_{Cr} = 0.41$ mol, $N_{TiCl_4} = 3.00$ mol, $N_{CH_4} = 1.00$ mol and $N_{H_2} = 200$ mol).

total reactions

$$TiCl_4(g) + CH_4(g) + H_2(g) \rightarrow TiC(s) + 4HCl(g) + H_2(g) \quad (1)$$

$$TiCl_4(g) + \tfrac{1}{2}N_2(g) + 2H_2 \rightarrow TiN(s) + 4HCl(g) \quad (2)$$

The total pressure during deposition was close to atmospheric. The $TiCl_4$ concentrations were varied from 0.5 to 3.0 vol %. The CH_4 and the N_2 concentrations were varied in the ranges of 1.0 to 2.0 vol % and 15 to 60 vol %, respectively. The samples were heated to the deposition temperature in an H_2 atmosphere. Linear gas flow velocity in the reactor was varied in the range of 1.2 to 2.8 m min^{-1}. Deposition time was normally one hour. Some nucleation experiments with short gas exposure, 5 to 15 min, were also carried out. These samples were used to study chlorination reactions at the surface at the begining of the deposition. Thicker coatings were used to study growth rates, interlayers, morphology and adherence of the coatings.

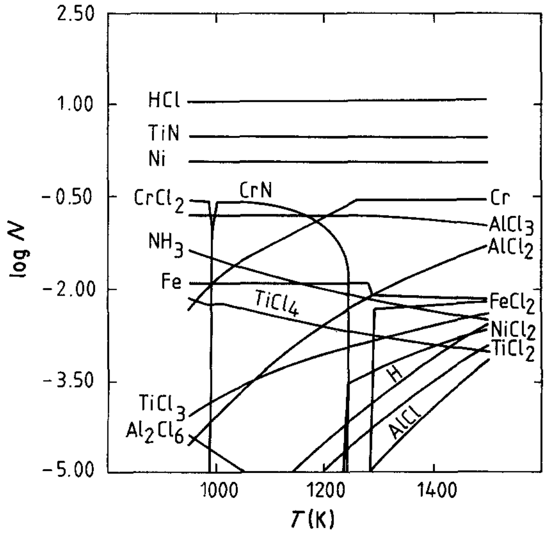

Figure 4 Yield of components as a function of temperature in the system TiN–MA 6000; $p = 1$ atm, gas excess in input reactants ($N_{Ni} = 1.15$ mol, $N_{Cr} = 0.29$ mol, $N_{Al} = 0.16$ mol, $N_{Fe} = 0.01$ mol, $N_{TiCl_4} = 3.00$ mol, $N_{H_2} = 130$ mol, $N_{N_2} = 70.0$ mol and $N_{H_2} = 130$ mol).

The substrate materials were the nickel-based alloy MA 6000 and the iron-based alloy Incoloy 800. MA 6000 has a γ matrix, which is strengthened by coherent γ' precipitates and Y_2O_3 dispersions. The other substrate material, Incoloy 800, has a γ structure. The compositions of these materials are listed in Table I. Incoloy specimens were cylinders with a diameter of 20 mm and a height of 5 mm. MA 6000 specimens were 5 mm × 15 mm plates with a thickness of 2 mm. Before deposition the substrates were polished and cleaned ultrasonically in acetone.

The microstructure of the coatings was studied by scanning electron microscope (SEM) and coatings were analysed by energy-dispersive spectrometry (EDS). Adhesion was tested by a scratch test.

4. Results and discussion

When the very first gas molecules meet the surface at the beginning of the deposition, the amount of metal components is high as compared with gaseous components, which obviously corresponds to the metal excess used in the thermodynamical calculations. After the surface is completely covered by the reaction products, the activity of the surface components with respect to the gas phase decreases. As the coating grows, the deposition situation corresponds more and more to the gas excess in the thermodynamical calculations.

It was found experimentally that even when the coatings had grown to 1 to 2 μm, the substrate materials still had an effect on growth rate. Otherwise it would be difficult to explain the thickness difference between coatings deposited with the same process parameters on MA 6000 (2 μm) and Incoloy 800 (1 μm)

If the calculations are performed having a metal excess in input reactants, the most reactive constituent of the substrate material dominates the reactions between gas phase and substrate. This may be in contradiction to the real situation, since it is probable that the most reactive constituent reacts first with the gas phase and, when these reactions are continued for a while, concentration of the constituent will decrease at the surface of the substrate. After that the other constituents also start to react with the gaseous reactants and the real situation at the growth boundary

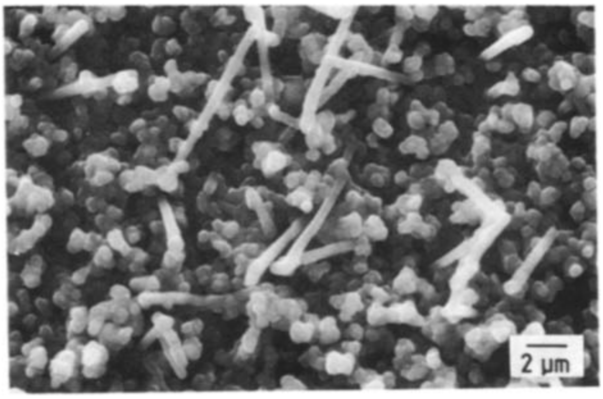

Figure 5 SEM micrograph of TiC deposit on MA 6000 in conditions at which formation of Ni_3Ti is favourable.

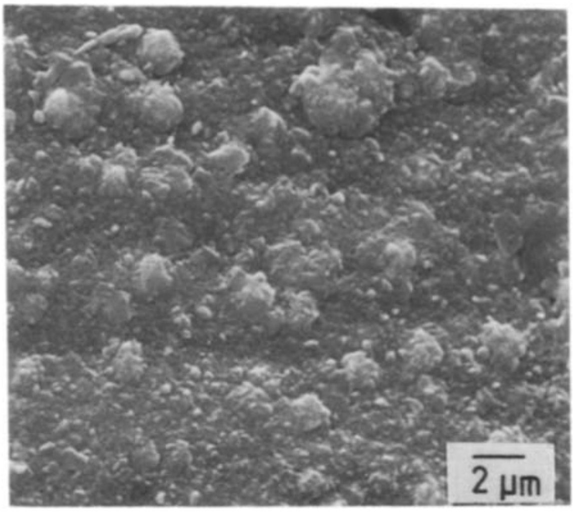

Figure 6 SEM micrograph of TiN coating on Incoloy 800.

rapidly begins to approximate more closely to the excess of gaseous components. From this point of view the role of the less reactive constituents might be better analysed if the calculations were performed having a gas excess in the input reactants instead of a metal excess. However, it has to be pointed out that whether the calculations are carried out having gas or metal excess in the input reactants, the calculations indicate the phases which can possibly form and they give an idea of the factors affecting the deposition of TiC and TiN on superalloys. So, the choice of the metal/gas ratio of inputs most of all affects the yields of the components.

4.1. TiC and TiN coatings on MA 6000

The adhesion of TiC coatings on MA 6000 was found to be very poor in cases where the formation of Ni_3Ti was promoted, i.e. if the $CH_4/TiCl_4$ ratio of input gases was low. This agrees with the results reported by Steinmann and Hintermann [9], who found that the adhesion of TiC–Ni_3Ti to nickel alloys is rather low.

Needle-like crystals, as shown in Fig. 5, were obtained in this study in those conditions where the formation of Ni_3Ti was possible. No Ni_3Ti interlayer was formed on Incoloy samples (under the same process conditions), so the needle-like crystal growth is induced by the substrate. If the coatings were deposited at high $CH_4/TiCl_4$ ratios, microstructurally dense coatings were obtained, but some porosity was observed in the coating–substrate interface. The explanation for this might be that under high excessive carbon conditions the surface is partially carburized at the beginning of deposition. Chlorination is concentrated in areas between carbide islands. The coating grows on these islands, and meanwhile localized chlorination makes pits between them. The pits are later covered by the coating.

The formation of Ni_3Ti in the system TiN–MA 6000 was found neither in the thermodynamical calculations nor experimentally. This disagrees with results reported by Erben *et al.* [10], who found experimentally a thin Ni_3Ti interlayer in the TiN–nickel-based superalloy system.

CVD TiC and TiN layers on MA 6000 were 1 to 2 times thicker than on Incoloy 800. The reason for this is that MA 6000 contains aluminium and other alloying elements which form very stable chlorides. At the beginning of deposition these elements increase the reduction of $TiCl_4$, which enhances nucleation and growth rates. The higher the H_2 content in input gases, the lower the difference in thickness between coatings on MA 6000 and Incoloy 800 was, i.e. the reducing effect of aluminium has a merely minor effect on growth when excess H_2 is present.

$CrCl_x$ clusters were found on the nickel-based alloy

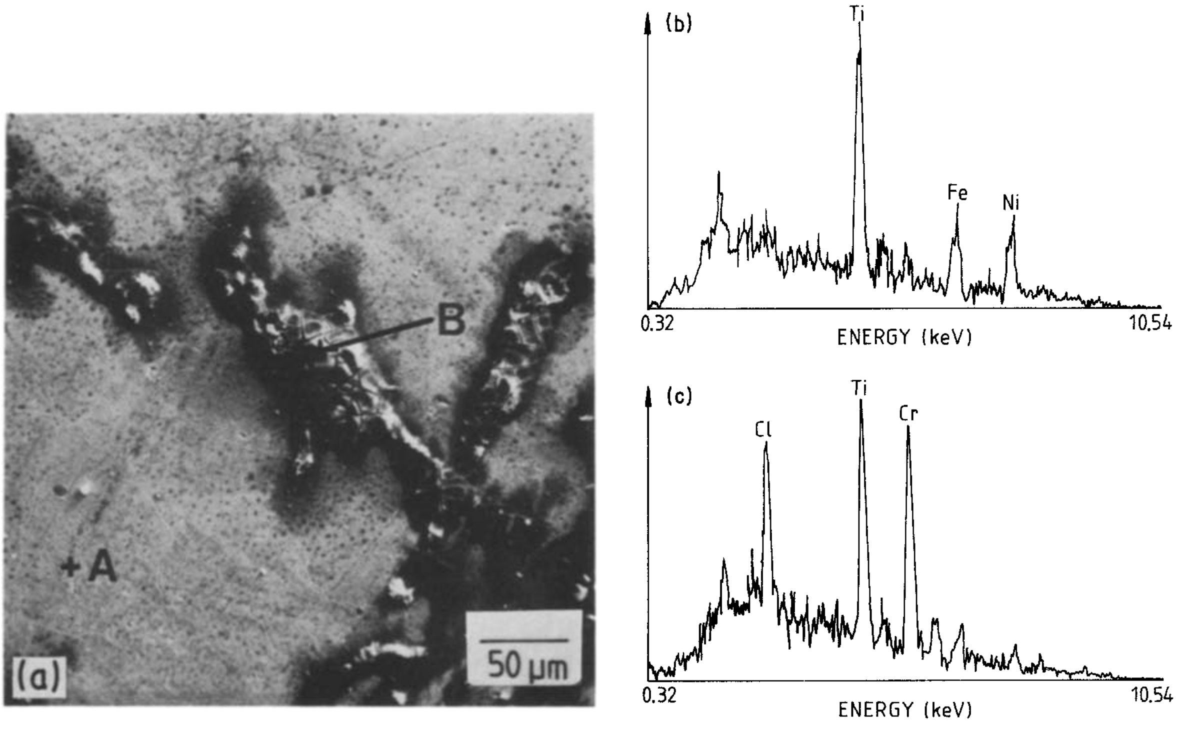

Figure 7 (a) SEM micrograph of $CrCl_x$ cluster on MA 6000, and EDS spectra of (b) the surface (Point A in Fig. 7a) and (c) the cluster (Point B). Deposition time is 15 min and deposition temperature 1023 K.

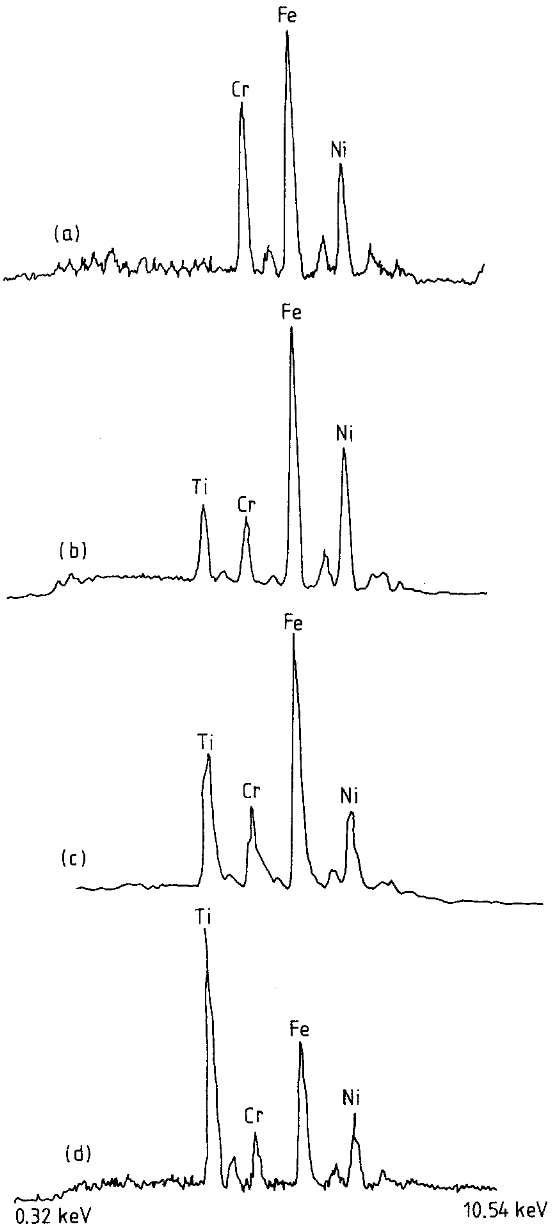

Figure 8 EDS spectra of TiN nucleation samples on Incoloy 800. (a) Incoloy 800 before deposition. (b) $T = 1193\,K$; $NiCl_2(s)$, $FeCl_2(l)$, $CrCl_2(l)$. (c) $T = 1263\,K$; $NiCl_2(g)$, $FeCl_2(l)$, $CrCl_2(l)$. (d) $T = 1333\,K$; $NiCl_2(g)$, $FeCl_2(g)$, $CrCl_2(l)$. $p = 1$ atm, $N_2 + 2.5$ vol % $TiCl_4$.

after nucleation experiments (deposited at low H_2 concentration). This can be explained in the case of TiN by assuming that at the beginning the formation of the TiN coating is controlled by the reduction of $TiCl_4$ by aluminium. This leads to a very thin porous TiN coating. As the aluminium content in the substrate decreases, chromium starts to chlorinate. This process leads to a mixture of TiN + liquid $CrCl_x$. $CrCl_2$ clusters that were observed in experiments on the surface by EDS were similar to those in Fig. 7.

4.2. TiC and TiN coatings on Incoloy 800

When TiN was deposited on Incoloy 800 at low H_2 concentration, porosity was observed at the interface between coating and substrate. The porosity was presumed to be caused by chromium and iron chlorination. The porosity of the interlayer could be decreased by decreasing the $TiCl_4$ concentration, by increasing the H_2/N_2 ratio or by nitriding the substrate before the deposition. The coatings deposited under high H_2/N_2 ratios appeared dense under microscope examination as shown in Fig. 6.

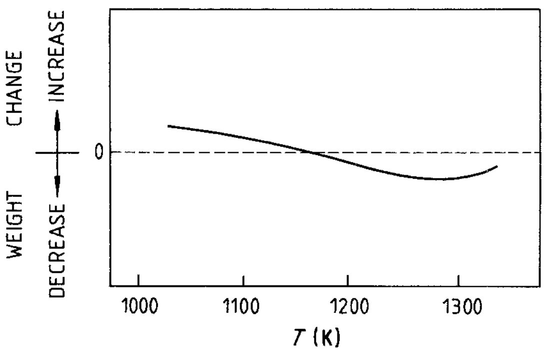

Figure 9 Weight changes of Incoloy 800 samples deposited at different temperatures. $CrCl_2(s) \rightarrow (l)$ at 1088 K, $NiCl_2(s) \rightarrow (g)$ at 1243 K and $FeCl_2(l) \rightarrow (g)$ at 1285 K.

According to the thermodynamical calculations the formation of liquid $CrCl_2$ is possible when the H_2/N_2 ratio is small. $CrCl_x$ clusters were observed experimentally as shown in Fig. 7.

The effect of deposition temperature on chlorination reactions is clearly shown in EDS spectra: when the deposition temperature increases from 1193 to 1263 K, nickel chloride transforms from solid to gaseous, which decreases the nickel intensity in the (b)EDS spectrum, and when the deposition temperature is increased to 1333 K, the $FeCl_2$ intensity is decreased relative to the intensities of $NiCl_2$ and $CrCl_2$, since $FeCl_2$ is gaseous at temperatures over 1285 K. Fig. 8 shows EDS spectra of TiN coatings on Incoloy 800 in the nucleation experiments. Iron and nickel chlorination was also observed as a weight loss of the Incoloy samples (after the weight of the coatings was excluded), as shown in Fig. 9.

5. Conclusions

The nickel-based alloy MA 6000 was found to be prone to the formation of Ni_3Ti during CVD of TiC. According to the thermodynamical calculations and deposition experiments the formation of this phase is favoured if

(a) the concentration of CH_4 is low,
(b) the concentration of $TiCl_4$ is high, or
(c) the concentration of H_2 is high.

If an Ni_3Ti interlayer is formed, it will destroy the adherence of the TiC coating and cause needle-like crystal growth.

Aluminium was found to have a great tendency to form chlorides. Faster growth rate on MA 6000 was explained by the fact that the reduction of titanium chloride is enhanced by elements in the substrate material which form stable chlorides.

When TiN is deposited on MA 6000 liquid $CrCl_2$ and liquid $FeCl_2$ can be formed. Traces of $CrCl_2$ were found by EDS.

The difficulty with CVD on Incoloy 800 was most of all interlayer porosity. This was explained to be caused by intense iron and chromium chlorination.

Thermodynamics does not explain the deposition process totally. Differences are caused by the fact that some of the reactions are kinetically limited, growth of the coating is not homogeneous, diffusion processes can dissolve or form interlayers during the growth period, and deposition depends on the transport of gaseous species from and to the surface (kinetic control by mass transfer or surface reactions). However, thermodynamical calculations, even though carried out on a semi-quantitative level, were shown to be good enough to predict the superalloy behaviour and explain some of the phenomena observed during CVD.

References

1. M. DUCARROIR, M. JAYMES, C. BERNARD and Y. DANIEL, *J. Less-Common Metals* **40** (1975) 173.
2. F. TEYSSANDIER, M. DUCARROIR and C. BERNARD, in Proceedings of the 3rd Euro-CVD Conference, edited by H. Hintermann (Laboratoire Suisse de Recherches Horloqeres, Neuchâtel, 1980) pp. 1–9.
3. L. VANDENBULCKE, *J. Electrochem. Soc.* **128** (1981) 1584.
4. M. REICHLE, Dissertation, Technische Universität Munchen (1971).
5. G. ERIKSON, *Chemica Scripta* **8** (1975) 100.
6. I. BARIN and O. KNACKE, "Thermochemical Properties of Inorganic Substances" (Springer, Berlin, 1973).
7. I. BARIN, O. KNACKE and O. KUBASCHEWSKI, "Thermochemical Properties of Inorganic Substances", Supplement (Springer, Berlin, 1977).
8. D. STULL and H. PROPHET, JANAF Thermochemical Tables, 2nd Edn (National Bureau of Standards, Washington, DC, 1971).
9. P. STEINMANN and H. HINTERMANN, *J. Vac. Sci. Technol. A* **3** (1985) 2394.
10. E. ERBEN, A. MUEHLRATZER, R. BERTINGER and H. ZEILINGER, in Proceedings of 8th International Conference on CVD, edited by J. Blocher, G. Vuillard and G. Wahl (The Electrochemical Society, Pennington, N.J., 1981) p. 664.

Received 23 September
and accepted 15 December 1986